23rd ABCM International Congress of Mechanical Engineering
December 6-11, 2015, Rio de Janeiro, RJ, Brazil

DISCRETE ROBUST CONTROLLER FOR QUADROTORS STABILITY

Adriano Frutuoso
IFAM Av. Danilo Areosa, 1672 – Distrito Industrial – Manaus - Amazonas
adriano.frutuoso@gmail.com

João Edgar Filho
UFAM Av. Gen. Rodrigo Octavio, 6200 – Coroado I – Manaus - Amazonas
joaoedgarc@gmail.com

André Henrique Santos
UFAM Av. Gen. Rodrigo Octavio, 6200 – Coroado I – Manaus - Amazonas
andrehls@hotmail.com

Abstract. *This paper approaches the angles stability control of a quadrotor. The vehicle parts (mechanical structure and electronic devices), dynamic modeling, controllers design methodology and the experimental results are also presented. Attitude controllers were designed using a PD/H_2 discrete control structure, which the gain of H_2 part was performed by solving a convex optimization problem, described in linear matrix inequalities form. The experiments indicate that angles dynamic responses can be changed by setting the gain of H_2, without modifying the gains of the proportional-derivative part. The results of PD/H_2 controllers were compared with a PD controller, in order to evaluate the overshoot and settling time.*

Keywords: *Quadrotor Stability, PD/H_2 Structure Control, Linear Matrix Inequalities*

1. INTRODUCTION

In recent years it has increased the number of UAVs (Unmanned Aerial Vehicles) projects for both military and civilian applications, due to the technological advances in data processing area and miniaturization of electronic and mechanical components (Bouabdalla *et al*., 2004).

Quadrotor UAV is a VTOL (Vertical Take-Off and Landing) vehicle composed of four rotors with simple mechanical structure (Suicmez and Kutay, 2014) and capable to fly in indoors and outdoors environments. The movements of quadrotor are illustrated in Fig. 1. Increasing or decreasing simultaneously the angular speed of the four motors, the quadrotor moves in a vertical axis. To move right, the speed of motor 4 is increased as compared to the motor 2 in order to tilt the quadrotor around the axis (2,4), while the rotations of motors 1 and 3 are increased to compensate the height loss. Similarly, it can move to left. Rotation movements around the vertical axis are performed by changing up, simultaneously, the rotation speed of motors 1 and 3 (rotate right) or 2 and 4 (rotate left).

The quadrotor stability control is not a trivial problem as it a suitable mathematical model that describes all or the main physical phenomena involved in its flight dynamic is necessary. Also, the quadrotor is a sub-actuated system so that the six degrees of freedom are controlled by only four control inputs (Raffo *et. al*., 2011). In addition, there are other problems related to stability control as degradation of signals sent by the inertial sensors, load limitation, restriction of movements that can perform by vehicle and the difficulty to implement the control algorithms, filtering and air navigation in embedded platform.

The objective of this paper is to design an embedded controller in a low-cost platform for quadrotor angular stabilization involving the structure and the tuning. Proposed controller for each angle of attitude has a combined PD/H_2 structure with two PD controllers and a H_2 controller in cascade. It is given special focus to the tune of H_2 controller held from the solution of an optimization problem presented on LMI (Linear Matrix Inequalities) form.

The use of LMI facilitates the design of state feedback controller for uncertain systems described as polytopic uncertainties. If the system to be controlled is known, the same solution using Riccati equation approach is obtained (Zhou *et al*., 1996). The dynamic response of the system can be adjusted with pole placement within a particular region of interest. These poles influence the transient and the steady state response of the system, making it faster or slower, with or without overshoot, for example. Poles placement can be described also as LMI problem (Chilali and Gahinet, 1996).

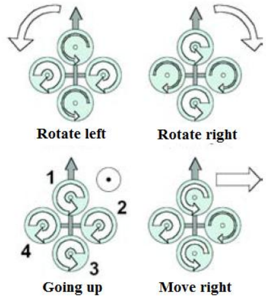

Figure 1. Examples of quadrotor movements (Bouabdallah, 2007).

2. DYNAMIC MODELLING AND SYSTEM ARCHITECTURE

2.1 Modelling

The body fixed frame *B* and the earth fixed frame *E* are illustrated in Fig. 2. The fixed frame *B* is used to represent the angular movements roll (ϕ), pitch (θ) and yaw (ψ) of quadrotor. The fixed frame *E* is used to represent the translational movements of quadrotor in the three dimensional space.

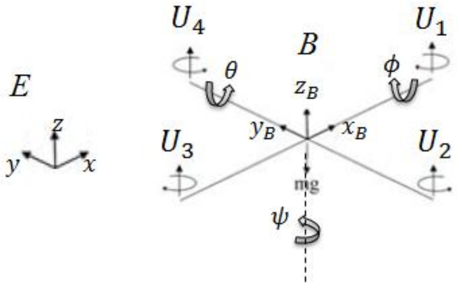

Figure 2: Body fixed frame *B* and earth fixed frame *E* representations. Adapted from Bouabdallah (2007).

The angular dynamic of quadrotor to hover conditions are given by Eq. (1) (Mellinger, 2012):

$$\begin{cases} \ddot{\phi} = \dfrac{I_{yy} - I_{zz}}{I_{xx}} \dot{\psi}\dot{\theta} + \dfrac{u_x}{I_{xx}} \\ \ddot{\theta} = \dfrac{I_{zz} - I_{xx}}{I_{yy}} \dot{\psi}\dot{\phi} + \dfrac{u_y}{I_{yy}} \\ \ddot{\psi} = \dfrac{I_{xx} - I_{yy}}{I_{zz}} \dot{\phi}\dot{\theta} + \dfrac{u_z}{I_{zz}} \end{cases} \tag{1}$$

where I_{xx}, I_{yy}, I_{zz} correspond to the moments of inertia about the x, y and z axes of *B*. The torques u_x, u_y, u_z around the *B* axes and are given by:

$$\begin{cases} u_x = l(U_2 - U_4) \\ u_y = l(U_1 - U_3) \\ u_z = (M_1 + M_3) - (M_2 + M_4) \end{cases} \tag{2}$$

where l is the distance from the axis of rotation of the rotors to the center of the quadrotor, U_i are the thrusts produced by the motors and M_i are the moments generated by the rotation of the propellers.

The dynamic model presented in Eq. (1) requires the knowledge of physical parameters such as I_{xx}, I_{yy}, I_{zz}. As the physical parameters of quadrotor used in this paper are unknown, empirical models obtained from black box system identification are used in the controllers designs whose dynamic responses of these models approximate to the real response as illustrated in Fig. 6.

2.2 Architecture

The quadrotor used in this paper consists of a frame (model X600), a propulsion system with brushless DC motors (BLDC) of 1000KV, four Electronic Speed Control (ESC) of 20A with a BEC of 2A and propellers of 9x4.7. Also, one Lipo 3000mAh 25-50C battery, a controller stability board and a communication module.

The essential part of system architecture is the controller board which is composed of an Arduino Nano V3.0, an inertial measurement unit MPU 6050, and connection pins for ESCs and Xbee communication module. In Fig. 3 it is illustrated the connection schematic. The microcontroller runs subroutines of communication with remote computer, angular stability control, communication with MPU 6050 and the generation of PWM signals used by ESCs.

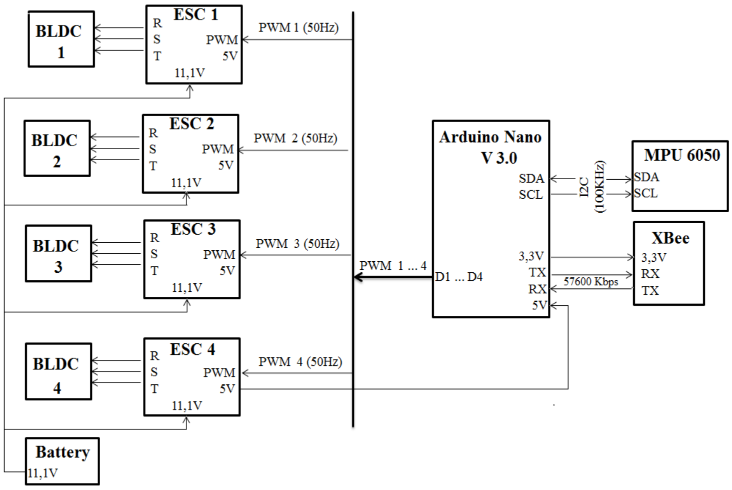

Figure 3. Schematic of Arduino Nano with ESCs, MPU 6050 and Xbee.

3. CONTROLLER PROJECT

3.1 Structure

The control structure of quadrotor is shown in Fig. 4. The blocks C_roll, C_pitch and C_yaw have combined PD/H_2 structure with two PD (Proportional-Derivative) controllers in cascade with an H_2 controller, Fig. 4 (b), wherein:

- C_gyro - PD controller of the angular velocity. It is responsible for stabilizing the angular velocity of axis attitude;
- C_acel - PD controller to zero reference. It is responsible for stabilizing the corresponding attitude axis in 0° position.
- C_r - H_2 controller. It changes the system dynamic response as performance specification.
- EST - estimator. This block performs the estimation of the states that will be feedback to C_r controller.

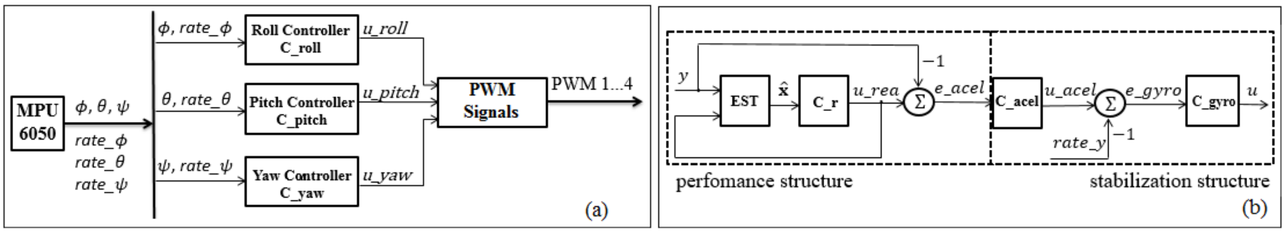

Figure 4. Quadrotor stability control. (a) Blocks diagram of attitude control. (b) Internal structure of C_roll, C_pitch and C_yaw.

The control signals *u*, *u_acel* and *u_rea* are given by Eq. (3), where *T* is the sample time, *y* is the attitude angle and *rate_y* is the angular variation on axis attitude. *Kp_gyro* and *Kp_acel* are proportional gains while *Kd_gyro* and *Kd_acel* are derivative gains of C_gyro and C_acel. The gain of C_r and the estimated states by EST are given by $\mathbf{K}$ and $\hat{\mathbf{x}}$ respectively.

C_acel and C_gyro are necessary for closed loop angular stabilization. Furthermore, this structure is used to obtain empirical models for each angle of attitude, since the quadrotor dynamics is unstable in open loop and this characteristic makes difficult the use of system identification techniques without a stabilization structure (Miller, 2011). The H_2 controller is used to set the dynamic response of the system without changing the gains of PD controllers.

$$\begin{cases} u(k) = \left(Kp\_gyro + \dfrac{Kd\_gyro}{T} \right) e\_gyro(k) - \dfrac{Kd\_gyro}{T} e\_gyro(k-1) \\ u\_acel(k) = \left(Kp\_acel + \dfrac{Kd\_acel}{T} \right) e\_acel(k) - \dfrac{Kd\_acel}{T} e\_acel(k-1) \\ u\_rea(k) = -\mathbf{K}.\hat{\mathbf{x}}(k) \\ e\_gyro(k) = u\_acel(k) - rate\_y(k) \\ e\_acel(k) = u\_rea(k) - y(k) \end{cases} \tag{3}$$

3.2 Tuning

The controller blocks C_roll, C_pitch and C_yaw are tuned in four steps. The first step is to affixe the attitude axis perpendicular to the axis that will be controlled. For the yaw angle, the central part of quadrotor is affixed. The second step is to define the gains of C_gyro in order to stabilize the angular velocity. After that, C_acel tuning is performed in order to stabilize the attitude angle at the reference position. Using the gains of C_acel and C_gyro, the tuning of C_r and EST are performed through the choice of **K** and **L**, respectively.

The gains of C_gyro define the dynamic behavior of the angular velocity on the attitude axis, excluding the effects of C_r, C_acel and EST. *Kd_gyro* can be changed to improve the system response time, making the controller more sensitive to speed variations. *Kp_gyro* is set to increase the compensation realized by the controller so that the angular speed becomes close to zero.

The C_acel tuning is performed based on the attitude angle response in closed loop, taking into account the gains of C_gyro obtained for angular velocity stability. Therefore, empirical tuning methods in closed loop can be used as the methods of Ziegler-Nichols or Tyreus-Luyblen (Al-Younes, 2009).

The C_r tuning is performed by choosing the gain **K**. This gain is obtained from the resolution of a convex optimization problem presented in LMI form. Therefore, consider the convex optimization problem given by Eq (4):

$$\min Tr[\mathbf{J}] \text{ with } \mathbf{X} = \mathbf{X}^T, \mathbf{J} = \mathbf{J}^T, \mathbf{Z}$$

$$\begin{cases} \begin{bmatrix} \mathbf{X} & \mathbf{B}_w \\ \mathbf{B}_w^T & \mathbf{J} \end{bmatrix} > 0 \\ \begin{bmatrix} -r\mathbf{X} & \mathbf{AX} + q\mathbf{X} \\ \mathbf{XA}^T + q\mathbf{X} & -r\mathbf{X} \end{bmatrix} < 0 \\ \begin{bmatrix} \mathbf{X} & \mathbf{XA}^T + \mathbf{Z}^T\mathbf{B}^T & \mathbf{XC}^T + \mathbf{Z}^T\mathbf{D}^T \\ \mathbf{AX} + \mathbf{BZ} & \mathbf{X} & \mathbf{0} \\ \mathbf{CX} + \mathbf{DZ} & \mathbf{0} & \mathbf{I} \end{bmatrix} > 0 \end{cases} \tag{4}$$

where **J** and **X** are symmetric and positive definite matrices, **Z** is an auxiliary rectangular matrix, **I** is the identity matrix, *Tr* [.] is trace operator of a matrix, *q* and *r* are, respectively, the center and the radius of the circle delimiting the allocation area of the poles of the feedback system. As **Z** = **KX**:

$$\mathbf{K} = \mathbf{ZX}^{-1} \tag{5}$$

The matrices **J**, **X** and **Z** are solutions of Eq. (4), and each LMI is a restriction to be served by the search algorithm of possible solutions to the problem. In case of Eq. (4), the restrictions are related to the Lyapunov stability condition for closed loop discrete system, the poles placement in a region of *Z* plan which define the dynamic response of the system, and the calculation of the H_2 norm from gramian observability.

The matrices **A**, **B**, $\mathbf{B}_w$, **C** and **D** are the state space model of the attitude angle and can be obtained using Euler-Lagrange or Newton-Euler formalism, since physical parameters of quadrotor required for modeling are known. As the physical parameters of quadrotor are not known, it is possible to obtain an empirical model for the attitude angle of interest using black box system identification (Stanculeanu and Borangiu, 2011). In this type of modeling, the model is obtained from observation of the system output behavior for a given input. Therefore, consider the discrete state space model in Eq. (6):

$$\begin{aligned}\mathbf{x}(k+1) &= \mathbf{A}\mathbf{x}(k) + \mathbf{B}u(k) + \mathbf{B}_w w(k)\\ y(k) &= \mathbf{C}\mathbf{x}(k) + \mathbf{D}u(k)\end{aligned} \tag{6}$$

The matrices of Eq. (6) are obtained considering the diagram in Fig. 5. A low intensity disturbance is applied at the end of the attitude axis of interest and gathering up *u* and *y* responses. With a computational tool for identification systems, like *Ident* available in Matlab, obtains a difference equation model with ARX (*Autoregressive with Exogenous inputs*) structure (Ljung, 1999) to the response of attitude angle, as shown in Eq. (7). From Eq. (7), the model presented in Eq. (6) is obtained using the discrete transfer function from *u* to *y*.

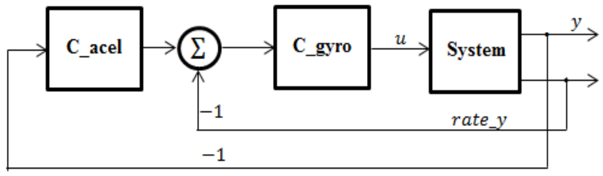

Figure 5. Model identification scheme to the attitude angle *y*.

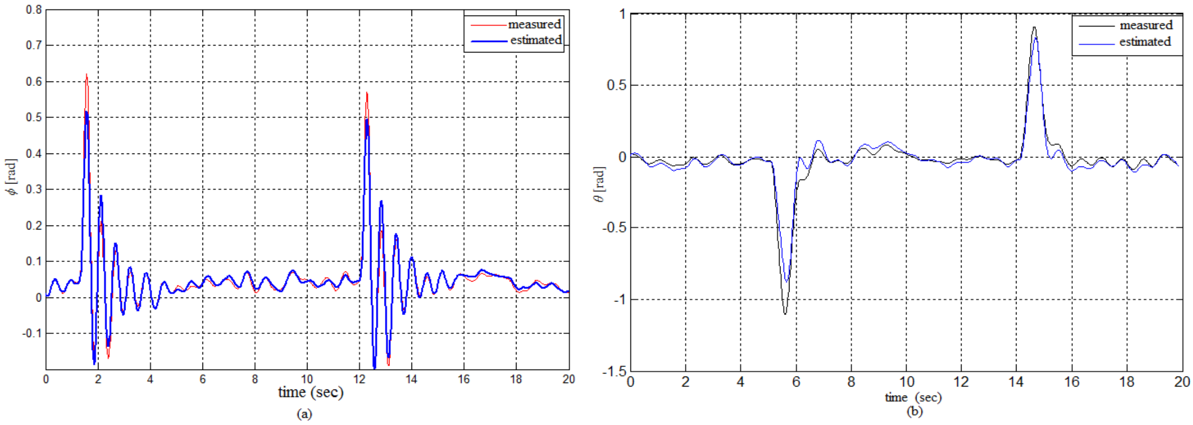

Figure 6. Comparison between the measured and estimated output using the ARX model with two poles and one zero (a) roll (b) pitch.

$$y(k) = \frac{B(q)}{A(q)}u(k) + \frac{1}{A(q)}v(k) \tag{7}$$

The EST block, Figure 7, is necessary to estimate variables of interest (states) that cannot be measured directly by sensors of quadrotor. The dynamic error between real and unavailable states and $\hat{\mathbf{x}}$ is given by Eq. (8). The dynamic error can be changed by $\mathbf{L}$. The relationship between $\mathbf{L}$ and the eigenvalues for desired dynamic error is presented in Eq. (9), where $\mathbf{F}$ contains the desired eigenvalues for dynamic error, $\mathbf{T}$ is a Lyapunov matrix and $\mathbf{L}_0$ is an arbitrary auxiliary matrix. The gain $\mathbf{L}$ is given by Eq. (10) (Chen, 1999).

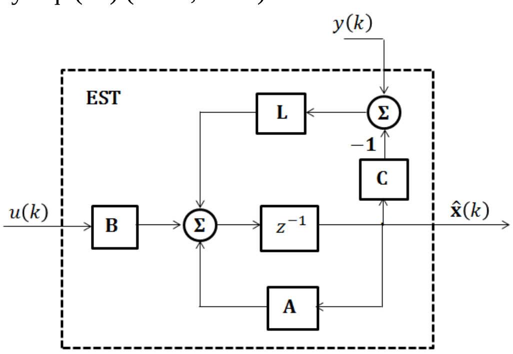

Figure 7. Estimator block (Luenberger observer).

$$\mathbf{e}(k+1) = [\mathbf{A} - \mathbf{L}\mathbf{C}]\mathbf{e}(k) \tag{8}$$

$$\mathbf{T}\mathbf{A} - \mathbf{F}\mathbf{T} = \mathbf{L}_0\mathbf{C} \tag{9}$$

$$\mathbf{L} = \mathbf{T}^{-1}\mathbf{L}_0 \tag{10}$$

4. EXPERIMENTS AND RESULTS

This section presents the results of experiments related to the stability control of the attitude angles. Overshoot and settling time were evaluated for two experiments: nonzero initial conditions and external disturbance.

Overshoot was measured from the highest peak exceeding the reference. The settling time was measured from the time that the response of the attitude angle remains within a variation range of +/- 5º in relation to the reference.

The results obtained for proposed structure control were compared with a PD control. In all experiments the sampling time was T = 20ms and control signals were limited within +/- 0.3 and the tuning gains are presented in Tab. 1.

Table 1. Gains of C_acel, C_gyro and EST for roll, pitch and yaw.

Gains	Roll and Pitch	Yaw
Kp_acel	0.2	0.25
Kd_acel	0	0.025
Kp_gyro	0.1	0.1
Kd_gyro	0.02	0.02
L	$[-3.7733 \;\; -3.9799]^T$	$[-5.2520 \;\; -5.4918]^T$

4.1 Roll

The experiments for roll angle were performed considering the gains of C_acel, C_gyro and EST shown in Tab.1, and the state space model is given in Eq. (11). Figure 8 shows the dynamic response using PD/H_2 and PD controllers. Overshoot and settling time obtained from nonzero response and external disturbance are presented in Tab. 2.

$$\begin{aligned}\mathbf{x}(k+1) &= \begin{bmatrix} 1.6960 & -0.7089 \\ 1 & 0 \end{bmatrix}\mathbf{x}(k) + \begin{bmatrix} 1 \\ 0 \end{bmatrix}u(k) + \begin{bmatrix} 1 \\ 1 \end{bmatrix}w(k) \\ y(k) &= \begin{bmatrix} -0.1166 & 0.0487 \end{bmatrix}\mathbf{x}(k) - 0.0688u(k)\end{aligned} \quad (11)$$

Table 2. Overshoot and settling time obtained for roll.

PD/H_2			Nonzero initial condition (ϕ = 50º)		External disturbance	
Q	*r*	**K**	M_p (deg)	t_a (sec)	M_p (deg)	t_a (sec)
-0.95	0.05	[-0.1935 0.1861]	-12.96	0.64	49.47	1.34
-0.75	0.05	[0.1989 -0.1461]	-3.46	0.4	41.48	1.38
-0.5	0.05	[0.7098 -0.4633]	0	0.9	38.18	0.9
-0.25	0.05	[1.2306 -0.6526]	0	6.92	39.66	1.06
0.0	0.05	[1.6919 -0.7085]	0	9.42	35.07	1.8
PD			-10.64	1.22	39.37	1.64

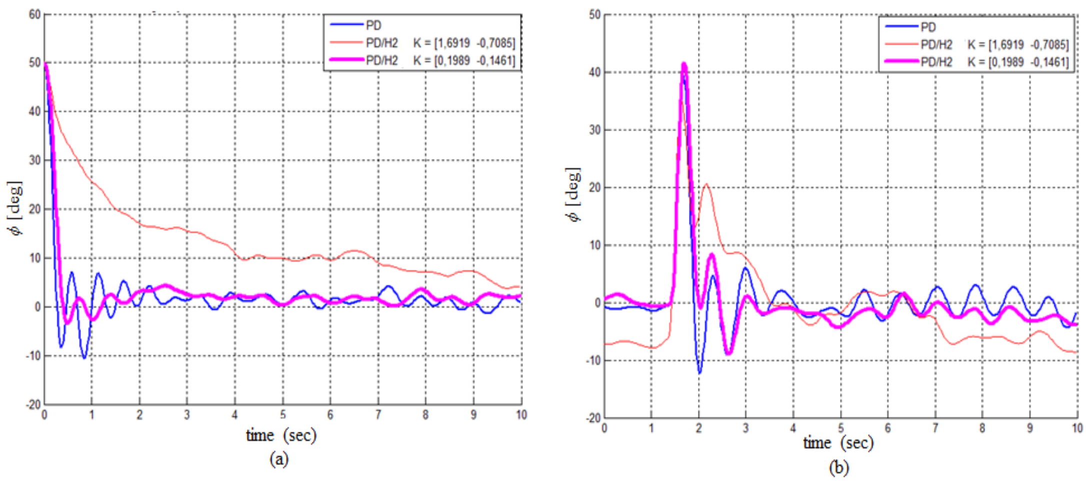

Figure 8. Comparative graphs between PD and PD/H_2 to ϕ (roll). (a) nonzero initial condition test (ϕ = 50º). (b) external disturbance test.

4.2 Pitch

For pitch angle, the same gains of Tab. 1 and the same state space model of roll were adopted since the structure of the quadrotor was considered symmetrical. Comparative plots are illustrated in Fig. 9 and overshoot and settling time are shown in Tab. 3.

Table 3. Overshoot and settling time for pitch.

PD/H$_2$			Nonzero initial condition (θ = -50º)		External disturbance	
q	*r*	**K**	M$_p$ (deg)	t$_a$ (sec)	M$_p$ (deg)	t$_a$ (sec)
-0.95	0.05	[-0.1935 0.1861]	17.52	0.62	-44.88	0.86
-0.75	0.05	[0.1989 -0.1461]	8.72	0.58	-48.99	0.6
-0.5	0.05	[0.7098 -0.4633]	0	0.4	-37.6	0.58
-0.25	0.05	[1.2306 -0.6526]	0	0.92	-45.8	1.28
0.0	0.05	[1.6919 -0.7085]	Undefined	>10	-47.14	>10
PD			20.85	0.74	-46.18	0.98

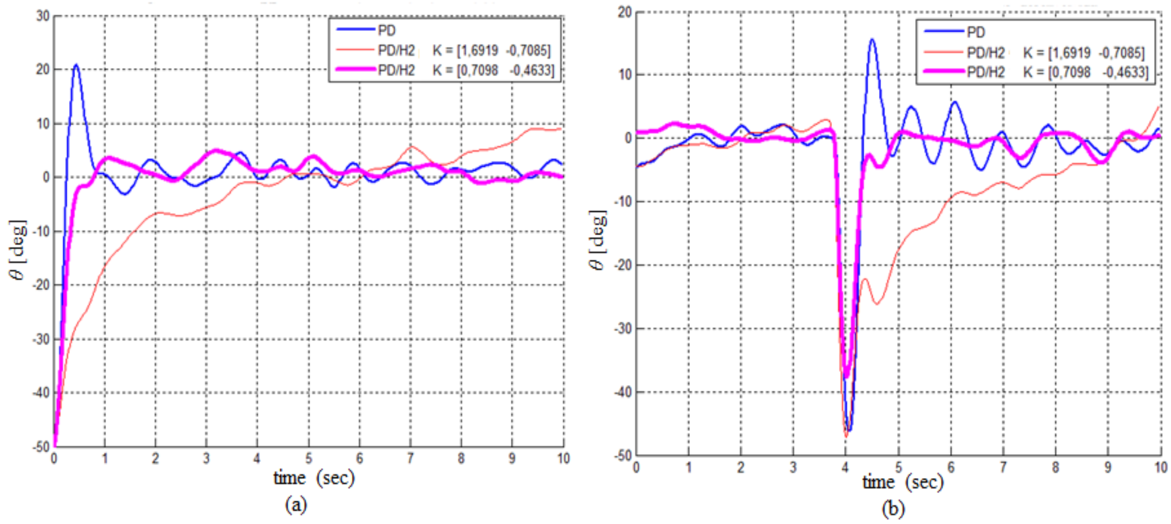

Figure 9. Comparative graphs between PD and PD/H$_2$ to θ (pitch). (a) nonzero initial condition test (θ = -50º). (b) external disturbance test.

4.3 Yaw

The results for yaw are presented in Tab. 5 and the dynamic responses graphs are illustrated in Fig. 10. The experiments were carried out considering the gains in Tab. 1 and the state space model given by Eq. 12.

$$\mathbf{x}(k+1) = \begin{bmatrix} 1.7890 & -0.8014 \\ 1 & 0 \end{bmatrix}\mathbf{x}(k) + \begin{bmatrix} 1 \\ 0 \end{bmatrix}u(k) + \begin{bmatrix} 1 \\ 1 \end{bmatrix}w(k)$$
$$y(k) = \begin{bmatrix} -0.0856 & 0.0383 \end{bmatrix}\mathbf{x}(k)\text{-}0.0478.u(k) \tag{12}$$

Table 4. Overshoot and settling time for yaw.

PD/H$_2$			Nonzero initial condition (ψ = -50º)		External disturbance	
q	*r*	**K**	M$_p$ (deg)	t$_a$ (sec)	M$_p$ (deg)	t$_a$ (sec)
-0.95	0.05	[-0.1005 0.0936]	14.81	4.42	-35.57	4.3
-0.75	0.05	[0.2919 -0.2386]	17.28	8.8	-29.39	7.18
-0.5	0.05	[0.8028 -0.5558]	7.44	>10	-46.54	>10
-0.25	0.05	[1.3236 -0.7451]	8.72	>10	-43.36	>10
0.0	0.05	[1.7845 -0.8007]	Undefined	Undefined	-62.02	Undefined
PD			23.2	3.22	-36.64	3.7

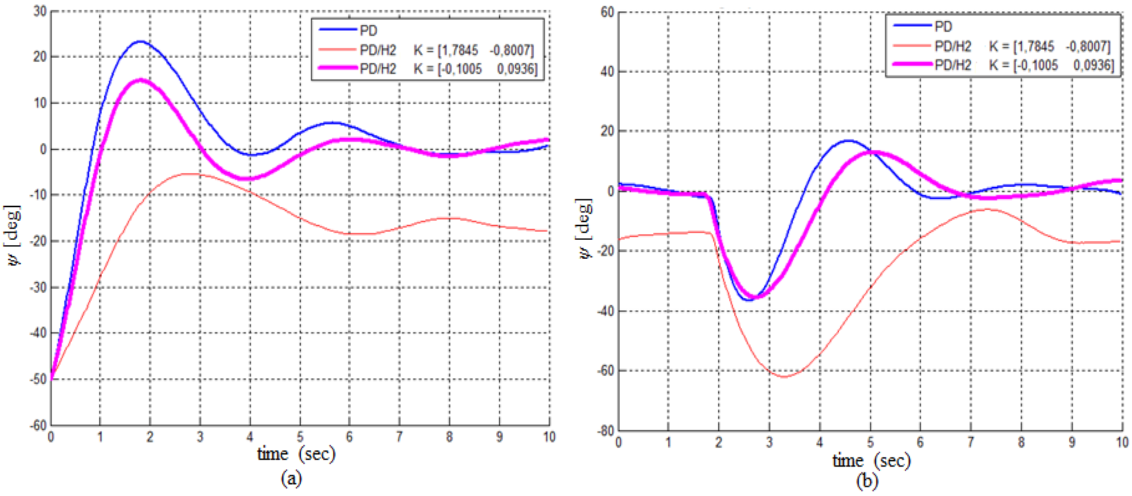

Figure 10. Comparative graphs between PD and PD/H_2 to ψ (yaw). (a) nonzero initial condition test (ψ = -50º). (b) external disturbance test.

5. CONCLUSION

This paper presented an alternative approach to controller design for quadrotor stability. It was used discrete feedback control theory witch the gain was obtained from the solution of an optimization problem presented in LMI form. Empirical black box modeling was used in the controllers design to obtain discrete models that describe the dynamics of the attitude angles. Such models were suitable, serving as an alternative to models obtained from classical formulation.

The experimental results showed that the design approach is feasible and presents satisfactory results in relation to overshoot and settling time for the tests performed, in special for roll and pitch angles. Future works includes control design to uncertain systems (with mass and rotational inertia variation) and adding integral action in the attitude controllers to enable stabilization in different angles and rejecting low intensity permanent disturbance.

6. REFERENCES

Al-Younes, Y., 2009. *Establishing Autonomous Aus-Quadrotor*. Thesis. American University of Sharjah, Sharjah.

Bouabdallah, S., 2007. *Design and Control of Quadrotors with Application to Autonomous Flying*. Thesis, EPFL, Lausanne.

Bouabdallah, S., Murrieri, P. and Siegwart, R., 2004. "Design and Control of an Indoor Micro Quadrotor". In: *Proceedings of IEEE International Conference on Robotics and Automation*. New Orleans, USA.

Chen, C.-T., 1999. *Linear System Theory and Design*. Oxford University Press, New York, 3rd edition.

Chilali, M. and Gahinet, P., 1996. "H∞ Design with Pole Placement Constraints: An LMI Approach". *IEEE Transactions On Automatic Control*, Vol. 41, p. 358 – 367.

Mellinger, D., 2012. *Trajectory Generation and Control for Quadrotors*. Ph.D. thesis, University of Pennsylvania, Philadelphia.

Miller, D. S., 2011. *Open Loop System Identification of a Micro Quadrotor Helicopter from Closed Loop Data*. Thesis. University of Maryland.

Ljung, L.,1999. *System Identification:Theory for the User*. Prentice Hall, New Jersey, 2^{nd} edition.

Raffo, G. V., Ortega, M. G. and Rubio, F. R., 2011. "Path Tracking of a UAV via an Underactuated H∞ Control Strategy". *European Journal of Control*, p.1-20.

Stanculeanu, I. and Borangiu, T., 2011. "Quadrotor Black-Box System Identification". World Academy of Science, Engineering and Technology. 08 Jul. 2014 <http://waset.org/publications/15465/quadrotor-black-box-system-identification>.

Suicmez, E.C. and Kutay, A.T, 2014. "Optimal Path Tracking Control of a Quadrotor UAV". In: *Proceedings of International Conference on Unmanned Aircraft Systems (ICUAS)*. Orlando, USA.

Zhou, K., Doyle, J.C. and Glover, K., 1996. *Robust and Optimal Control*. Prentice Hall, New Jersey.

7. RESPONSIBILITY NOTICE

The authors are the only responsible for the printed material included in this paper.